2015

Nanocluster Thin-Films for Sensor Applications

Joseph Serritella
University of Central Florida

NANOCLUSTER THIN-FILMS FOR SENSOR APPLICATIONS

by

JOSEPH SERRITELLA

A Thesis submitted in partial fulfilment of the requirements
for the Honors in the Major Program in Electrical Engineering
in the College of Engineering and Computer Science
and in The Burnett Honors College
at the University of Central Florida
Orlando, Florida

Spring Term 2015

Thesis Chair: Dr. Donald C. Malocha

Abstract

The ability to sense gas such as methane can provide an early warning system to protect human lives. High demand for the ability to sense the world around us has provided an extensive area of research for sensor technology. In particular, current sensor technology, specifically for methane, has provided sensors that require a heated environment to function. The majority of current methane sensors function at temperatures between 150°C and 450°C [1-3]. This thesis will explore an approach to produce a room temperature methane sensor.

This research will investigate techniques to create a sensor that is responsive to methane at 23°C. The approach will use the integration of a very thin film, which changes its resistive properties when methane gas is applied, deposited atop the surface of a piezoelectric substrate. An aluminum thin film interdigital transducer will launch a surface acoustic wave (SAW) that travels under the sensor's gas-sensitive resistive thin film. The SAW/resistive film interaction changes the SAW amplitude, phase and delay. For this work, three films, tin dioxide (SnO_2), zinc oxide (ZnO) and palladium (Pd) [1, 2] will be studied. Gas detection will be shown when combining ZnO and Pd, and, observable change in SAW propagation loss is measured when methane gas is present at the film.

Dedication

To my family and friends that always stood by my side throughout life, you have motivated me, inspired me, and taught me to believe in myself. To everyone that lost a loved one before they were ready and to my beloved Grandfather, Alfred Giordano.

Acknowledgments

I would first like to thank everyone that helped me though my career here at the University of Central Florida. This project was completed under the direction of Dr. Donald C. Malocha and Dr. Brian Fisher, without their help this would have never been finished. This was also made possible by all the graduate students belonging to CAAT. During my time here at UCF I had the privilege to study for my last two years of undergraduate school under Dr. Malocha, without this experience I would have never found a love for Electrical Engineering. I am so grateful for his guidance and inspiration.

To my Thesis Committee members, Dr. Weeks, Dr. Flitsiyan, and Dr. Wahid, you have made my time here so wonderful and I couldn't have been happier to learn from you. I truly appreciate your time and energy.

Finally, thank you to my grandfather for making who I am today.

Table of Contents

Table of Figures

Chapter 1 Introduction

Solid state gas sensors developed with SnO_2 or ZnO have been researched over many decades [21]. Current solid state sensors have become principle as gas alarms, both domestic and industrial [2, 4]. In particular, current sensor technology, specifically for methane, has provided sensors that require a heated environment to function. With majority of these sensors functioning at temperatures between 150°C and 450°C [1-3]. Extending the temperature range to 23°C will expand the application of methane sensors. Proposed research will elaborate upon solid state devices that have demonstrated sensitivity to hydrogen gas at 23°C [4].

This research will investigate techniques to produce a room temperature methane sensor. One technique is to deposit a thin film, which changes its resistive properties when methane gas is applied, atop the surface of a piezoelectric substrate. Fabrication of an interdigital transducer (IDT) will generate a surface acoustic wave (SAW) that travels under the gas-sensitive resistive thin film. The SAW/thin-film interaction will change the wave's velocity, delay, and amplitude. This approach studies three thin films; tin dioxide (SnO_2), zinc oxide (ZnO) and palladium (Pd). By monitoring changes in wave properties gas presence at the film can be extracted.

Chapter 2 will provide a general overview of SAW technology along with presenting a reflective delay line. In chapter 3, theory behind the SAW/thin-film interaction will be evaluated. Furthermore, calculations will provide a detailed plot of SAW attenuation on a piezoelectric versus surface film sheet resistivity.

Film deposition on a 50MHz reflective delay line device will be discussed in chapter 4. Experimentation presented will analyze the SAW/thin-film interaction when methane gas is

present at the film. A relationship to film thickness and gas detection is also given in this chapter. An experiment determining ZnO cross sensitivity to hydrogen gas was also conducted and the results are included in chapter 4.

Chapter 2 SAW Background

Surface acoustic wave (SAW) devices have been researched for over 50 years. One such application is their use as bandpass filter elements in radar systems and televisions [6]. As sensors, SAW devices have been demonstrated to detect environment variables such as temperature, liquid levels, and mechanical stresses. SAW sensors can operate wirelessly and passively, which demonstrates an advantage over wired sensing solutions [5].

A SAW is a mechanical traveling wave trapped within one wavelength of a piezoelectric substrate. The SAW is generated by an applied electric field onto an interdigital transducer (IDT), which is fabricated atop a piezoelectric substrate. The IDT generates a periodic electrical signal on the piezoelectric, in turn, the piezoelectric properties create mechanical stresses in the substrate. The mechanical stress resonates at the frequency of the applied field, which generates the acoustic wave [6]. The anatomy of a SAW device is depicted in figure 2-1.

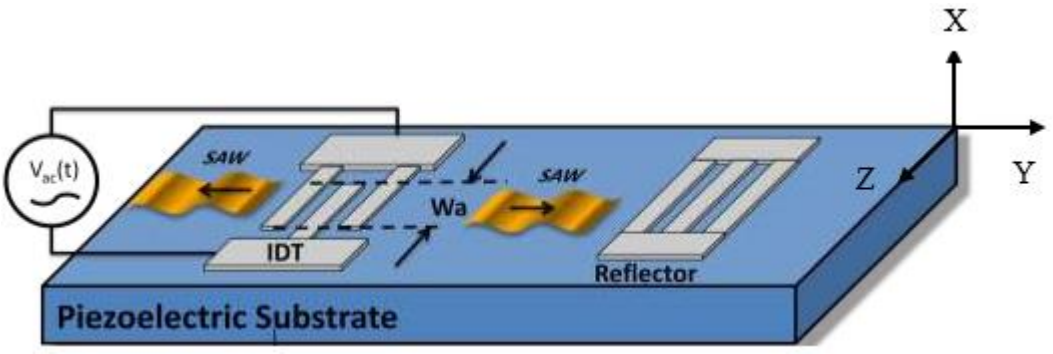

Figure 2-1: Interaction between the IDT, wave (beam width Wa) and reflector. An electric field of frequency f is applied to the IDT. As a result the piezoelectric effect generates a mechanical wave at frequency f. The acoustic wave propagates bidirectionally until contact with a reflector, where the wave is reflected back. to the IDT. [7].

Figure 2-1 shows the mechanical wave generated by applying an electric field of frequency *f* at the IDT. As a result the piezoelectric effect generates a mechanical wave of beam width *Wa*. The SAW propagates bidirectionally along the Y-axis until encountering a reflector, where the wave is reflected towards the IDT. The mechanical wave is received at the IDT, where a reciprocal process converts the mechanical stress into an electric signal.

2.1 SAW Delay Line

A reflective delay line consists of two surface elements, an IDT and a reflector. The SAW generated at the IDT propagates until it makes contact with a reflector. When the SAW encounters the reflector bank a portion of energy is reflected back to the IDT. The SAW delay, the time it takes to reach the reflector is $\tau_D = \frac{L_D}{V_{saw}}$, where L_D is the distance between the IDT and reflector and V_{saw} is the velocity of the acoustic wave. Figure 2-2 illustrates the reflective delay line used in the research.

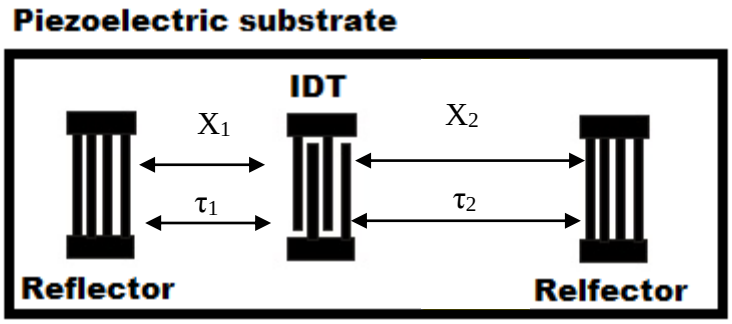

Figure 2-2: A SAW reflective delay line. The time delay between reflectors is τ and distance is given by X. Having τ_1 and τ_2 at different lengths the pulse delays are changed. The return signal from τ_1 is expected sooner than τ_2.

The delay line presented operates with two reflectors on either side of the IDT, each with a different distance from the IDT. The SAW makes contact with the closer reflector first, therefore return waves are received at the IDT at different times. For example, assuming X_1= 0.34cm and X_2=0.68cm with a SAW velocity of 3488 m/s, the time delays will measure τ_1=1 micro-second (μs) and τ_2=2μs. Accounting for wave travel time from the IDT to the reflectors and back, the waves are received by the IDT at 2μs and 4μs, which is known as the time response, plotted in figure 2-3.

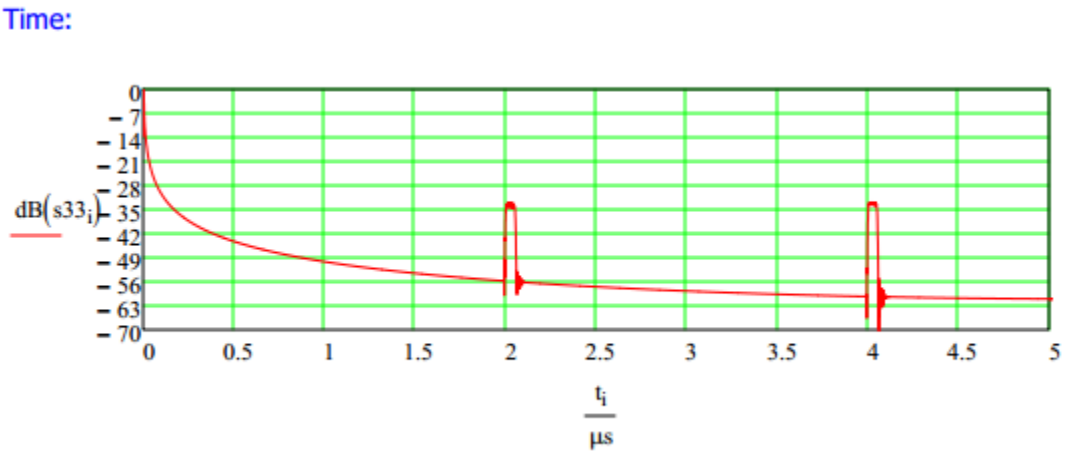

Figure 2-3: SAW time response plotted using MathCAD. Return waves are measured at 2μs and 4μs. 2μs refers to the closer reflector and 4μs represents the further reflector. Since each reflector is independent the return energy will be approximately the same, assuming no propagation loss.

Assuming no propagation loss, each wave has the same energy, because the reflectors are on either side of the IDT. Each transit is separated by 2μs, which prevents the transits from overlapping. Addition of a thin-film to the SAW propagation path will further alter the time response [7]. Chapter 3 will discuss the relationship between the SAW and thin-films in greater detail.

Chapter 3 SAW – Thin Film Analysis

Chapter 3 focuses on the surface acoustic wave's interaction with thin films developed. Changes of SAW's characteristics such as, propagation loss and group delay are measurable when the thin-film resistivity varies with gas concentration [7].

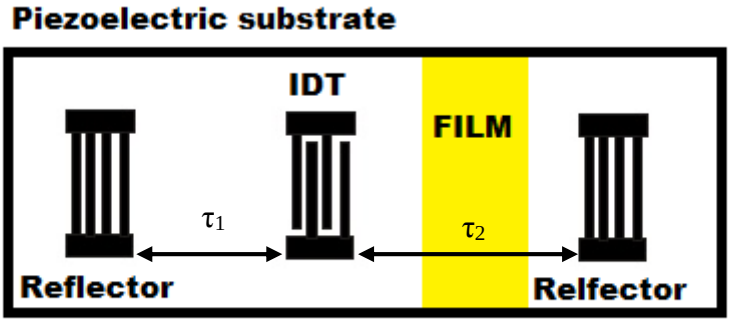

Figure 3-1: Thin-Film deposition between reflector and IDT in delay τ_2

Figure 3-1 show the deposited film in the acoustic path, separated by delay τ_2, interacting with the wave as it propagates from the transducer to the reflector and back to the transducer. The IDT and reflector response of this SAW delay line produces two separate time delayed responses. The return time delay of the first pulse reflection, τ_1, is given as $A_1 e^{-j\omega\tau_1}$ where A_1 is the magnitude of the wave and $e^{-j\omega\tau_1}$ is the delay. The return time delay of the second pulse reflection, τ_2, is given as $A_2 e^{-j\omega\tau_2}$ where A_2 is the magnitude of the wave and $e^{-j\omega\tau_2}$ is the delay. Ingebrigtsen has shown wave velocity and propagation loss varies as a function of the piezoelectric material and a surface film's resistivity [7]. A thin film's resistivity, R, changes, the SAW amplitude, A(α), which changes with respect to the attenuation constant α(R). In the

proposed work, the thin film deposited in the propagation path changes its resistivity as it is exposed to methane gas, and a change in the SAW propagation loss is expected.

The SAW mechanical and electric field wave equations are given as,

$$A(f,t) = A_0(f)e^{j(kx-\omega t)}, \quad (3\text{-}1)$$

where A_0 is the initial wave produced by the transducer as a function of frequency, f, and k is the propagation constant given by β+jα. β is the wave number 2π/λ and α is the propagation loss term. SAW wavelength is given as λ and the angular frequency, ω, is equal to 2πf. By substituting β+jα for "k" the wave equation can be rewritten as

$$A(f,t) = A_0(f)e^{-\alpha x}e^{j(\beta x-\omega t)}, \quad (3\text{-}1)$$

where the attenuation (propagation loss) is given by $e^{-\alpha x}$. As the film absorbs gas the resistivity varies, changing the attenuation constant α(R) and delay. Depending on the device embodiment, the SAW amplitude, phase, and delay are modified and can be used to extract the required parameters. For the case of gas sensing, the device insertion loss would be calculated versus the gas concentration of interest. Parameters such as path loss and phase change are determined by comparing the magnitudes and phases of the total reflection, which is given as

$$A = A_1e^{-j\omega\tau_1} + A_2e^{-j\omega\tau_2}, \quad (3\text{-}2)$$

As α(R) varies the magnitude and phase, "A_2" changes accordingly as:

$$A_2(x,f,t,R) = A_0(f)e^{-\alpha(R)x}e^{j(\beta x-\omega t)}, \quad (3\text{-}3)$$

As the resistivity changes, a difference in delay is measured by comparing the phases, given equation as.

$$\Delta\varphi(\omega) = \arctan\left(\frac{Im(A_1 e^{-j\omega\tau_1})}{Re(A_1 e^{-j\omega\tau_1})}\right) - \arctan\left(\frac{Im(A_2 e^{-j\omega\tau_2})}{Re(A_2 e^{-j\omega\tau_2})}\right), \quad (3\text{-}4)$$

The percent change in delay can be determined from the difference in the terms in 3-4. Change in wave amplitude can be extracted by comparing magnitude changes in dB given as.

$$\Delta A(\omega) dB = 20\log\left(\left|A_1 e^{-j\omega\tau_1}\right|\right) - 20\log(\left|A_2 e^{-j\omega\tau_2}\right|), \quad (3\text{-}5)$$

When exposed to a gas like methane the sheet resistance of the film changes in relation to gas presence [10] altering the attenuation constant. Assuming no mechanical losses due to the film the attenuation constant as a function of resistance is defined as [5].

$$\alpha(R_s) = -\left(\left(\frac{2\pi f K^2}{2V_{sc}}\right)\left(\frac{R_s V_{sc}\varepsilon_p}{1+(R_s V_{sc}\varepsilon_p)^2}\right)\right), \quad (3\text{-}6)$$

V_{sc} is the short circuit velocity of the wave, R_s is defined as sheet resistance of the film, and ε_p is the effective electrical permittivity of the film and K^2 is the acoustic coupling coefficient. The attenuation constant, α, is a function of $R_s \cdot V_{sc} \cdot \varepsilon_p$ when the term equals one, the electrical loss is at its greatest. As the sheet resistance tends towards infinity the SAW travels at the open circuit wave velocity Voc, similar to a substrate with no film in the propagation path. When the sheet resistance tends towards zero, the SAW travels at the short circuit wave velocity Vsc; similar to a metal in the propagation path. In either velocity case the acoustoelectric propagation losses are at a minimum. $R_s \cdot V_{sc} \cdot \varepsilon_p$ represents the ratio of film sheet resistance to the piezoelectric impedance. The piezoelectric impedance Z_p is the inverse of the substrate capacitive susceptance defined in as.

$$Z_p = \frac{1}{2\pi f_{sc}\varepsilon_p\lambda}, \tag{3-7}$$

By substituting $f_{sc}\lambda$ for V_{sc} in 3-7, the form is written as

$$R_s V_{sc}\varepsilon_p = \frac{R_s}{2\pi}\left(2\pi f_{sc}\varepsilon_p\lambda\right), \tag{3-8}$$

$$\frac{R_s}{2\pi}\left(2\pi f_{sc}\varepsilon_p\lambda\right) = \frac{R_s}{Z_p}\left(\frac{1}{2\pi}\right), \tag{3-9}$$

as Rs/Zp tends towards zero or infinity α(R) equals 0, which is the minimum value of α. As $R_s \cdot V_{sc} \cdot \varepsilon_p$ tends towards 1 α(R) equals $\frac{\omega K^2}{2V_{sc}}$, where the maximum energy is coupled into the film. Figure 3-2 plots the relationship between sheet resistivity and the attenuation constant of the wave for lithium niobate.

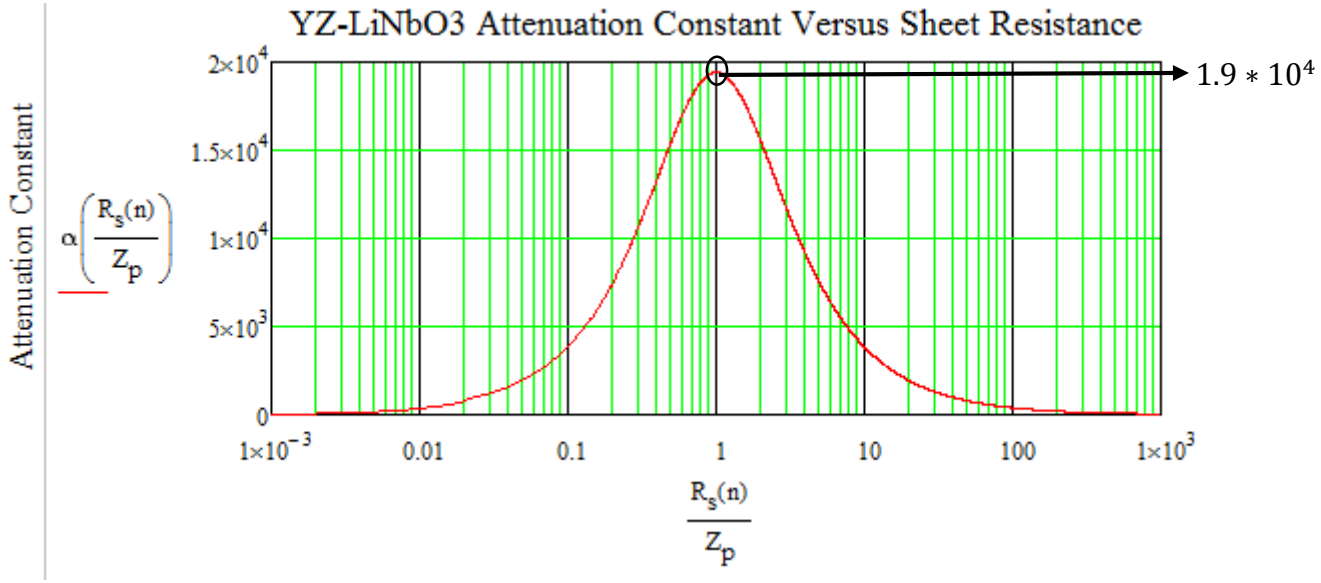

Figure 3-2: Acoustoelectric attenuation constant as a function of sheet resistance, velocity, and permittivity. Attenuation constant axis is in 1/m. Rs(n)/Zp is the ratio of varying film sheet resistance to the impedance of the piezoelectric.

For $LiNbO_3$ the maximum attenuation constant of $1.9*10^4$ m^{-1} occurs when the sheet resistance matches the impedance Z_p. As resistance varies the insertion loss of the SAW delay line can be measured. By gating the pulses and calculating change in delay and change in path loss gas absorption can be extracted. Specific films used and methodology for growth will be discussed in greater detail in the remaining sections of this chapter.

Chapter 4 Experiments

A methane sensor requires thin-film deposition onto the SAW's propagation path, which changes the SAW propagation loss characteristics as described in chapter 3. Experiments were performed to characterize each thin-film grown on a substrate, followed by experiments to determine the film's sensitivity to methane and cross-sensitivity to hydrogen gas. The goal was to measure and observe changes in SAW propagation loss when methane gas is present at the film. Multiple devices we fabricated to understand the SAW/thin-film interaction. Data and plots characterizing the behavior of the sensors were produced in these experiments.

4.1 Thin Film Depositions

Sensor fabrication requires the growth of two pairs of thin-films, either; ZnO and Pd or SnO_2 and Pd. Deposition methods such as the sol-gel method and RF sputtering have been demonstrated as effective methods for growing ZnO and SnO_2, however they are outside the scope of this research [2]. Therefore films were grown using a thermal evaporation system, known as electron beam evaporation. The Evaporation system used is shown in figure 4-1

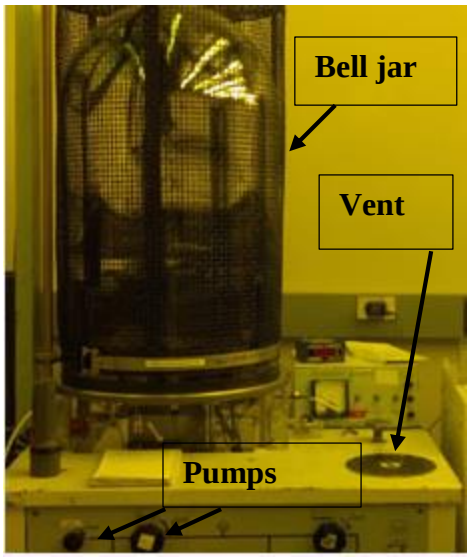

Figure 4-1: Electron beam evaporation system. A sample is placed inside of the bell jar, which is pumped to high vacuum. When high vacuum is reached, current is applied to a filament, which produces an electron beam. The beam is used to heat and melt the source material. The material evaporates filling the chamber, therefore coating the sample with a metal film.

The sample is placed inside a sealed bell jar known as the chamber. The chamber is pumped down to create a high vacuum, in the experimentations film deposition began at 5 μTorr. When high vacuum is reached, a source current was applied to a tungsten filament inside the chamber, creating an electron beam. The beam is directed at the crucible, where the source metal is held, which heats the metal until evaporation. When evaporated the chamber is filled with the source metal, in turn, coating the sample with the metal film. Thin film growth using the e-beam system is discussed in much greater detail in appendix B and C.

However, as shown in 3-1 film growth is limited to a small portion of the piezoelectric substrate. To achieve selective growth a shadow mask is used. The shadow masked was develop as in previous research experimentation [5]. The fixture allows for selective film deposition and measurements on the sensor. For deposition he SAW device is placed under the four probes and secured. The shadow mask is connected to the device's test fixture with a screw at each corner.

The device is then placed in the electron beam system for metal deposition. After metal deposition measurements on the sensor are made using a Vector Network Analyzer connected to the SMA port.

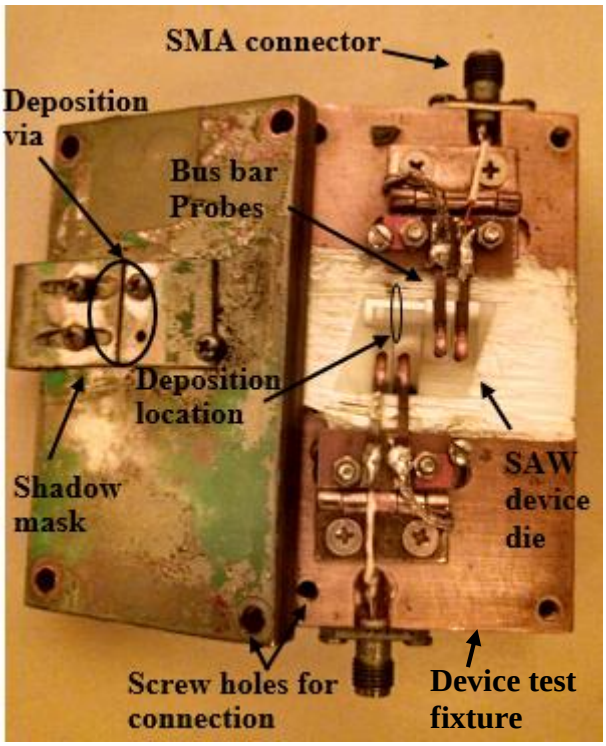

Figure 4-2: Picture of the test fixture and shadow mask for the 50MHz SAW device. The fixture is placed inside of the bell jar, when the material evaporates filling the chamber, only a portion is exposed to the material. The SAW device is placed under the metal probes and secured. Attaching the mask to the test fixture requires one screw per corner. Only a portion of the SAW device is exposed to the evaporated metal.

Once the desired film has been grown, it is necessary to anneal the film. The annealing process increases the resistivity of the material [8, 9]. The devices were placed in a glass petri dish and annealed in an air environment within a programmable furnace. The annealing temperature must be kept below 400°C in order to protect the aluminum electrodes from oxidizing [10]; 350°C is the set temperature to provide a buffer from the oxidation point. After

The Furnace was set to 30°C/min and required 12 minutes to reach 350°C. The soak time varied from 10 minutes to 24 hours. A picture of a 10 minutes anneal cycle is shown in figure 4-3.

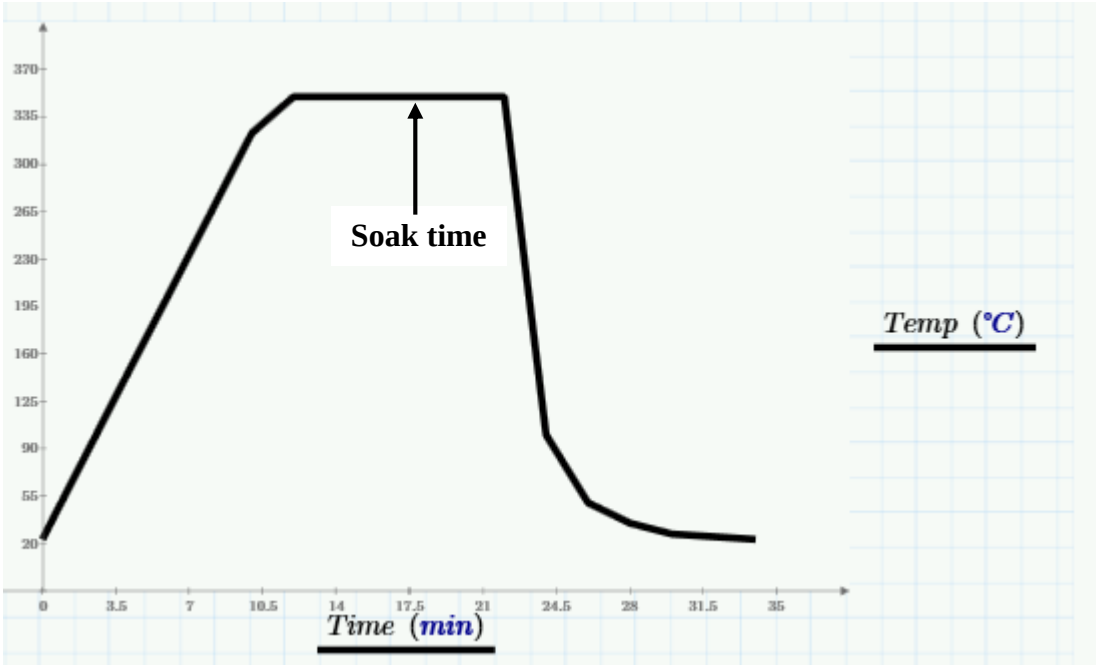

Figure 4-3: A graph of furnace temperature ramp, anneal and cool down time for the SAW methane sensor.

After completing the annealing process, the sensors are ready for testing.

4.2 Film Growth Parameters

The growth parameters for each metal deposited using the e-beam system are characterized in the following figures.

Parameter	
Material	SnO_2
Crucible line	Aluminum oxide
Filament current	8mA
Depostion rate	3 Å/s
Thickness	250 Å

Figure 4-4 Growth Parameters for a tin dioxide Film. SnO_2 was grown on YZ-LN using an e-beam system. Deposition occurs during a filament current of 8mA with a rate of 3 Å/s. The shutter was closed at 250 Å to stop the deposition.

The growth parameters for a tin dioxide thin film are given in figure 4-4. SnO_2 was grown on YZ-LN using an e-beam system. Deposition occurs during a filament current of 8mA with a rate of 3 Å/s. A low deposition rate allows for better monitoring and control of the film's thickness. The shutter was closed at 250 Å to stopping the deposition. The growth parameters for palladium are shown in figure 4-5.

Parameter	
Material	Pd
Crucible line	Aluminum oxide
Filament current	29mA
Depostion rate	0.1 Å/s
Thickness	20 Å

Figure 4-5 Growth Parameters for a palladium Film. PD was grown on YZ-LN. Deposition occurs at a filament current of 29mA with a rate of 0.1 Å/s. The shutter was closed at 20 Å to stop the deposition.

Pd was grown on YZ-LN using an e-beam system. Deposition began at a filament current of 29mA with a rate of 0.1 Å/s. Deposition was stopped when the thickness measured 20 Å on the crystal monitor. Zinc Oxide deposition in the electron beam system proved too difficult. A deposition rate and thickness were measured on the crystal monitor however, there was no film present at the substrate when measured using a profilimeter. To solve this issue zinc (Zn) was grown in the e-beam and then oxidized in a programmable furnace. The growth parameters for a zinc thin film are given in figure 4-6.

Parameter	
Material	Zn
Crucible line	Aluminum oxide
Filament current	4mA
Depostion rate	3.45 Å/s
Thickness	500 Å

Figure 4-5 Growth Parameters for a zinc Film. Zn was grown on YZ-LN using an e-beam system. Deposition occurs during a filament current of 4mA with a rate of 3.45 Å/s. The shutter was closed at 500 Å to stop the deposition.

Since the melting point of Zn is 491°C, deposition began at a filament current of 4mA with a rate of 3.45 Å/s. The lower melting point of zinc made control of the film's thickness and deposition rate extremely difficult.

4.3 Zinc Oxidation

Deposition of zinc oxide cannot be completed using electron beam evaporation. An extra step is needed to oxidize zinc. An experiment was created to measure the oxidation time of Zn on a silicon wafer. Positive photo-resist was applied to the wafer in the size of a dime and baked, then placed in the thermal evaporation system. Once removed from the system, the PR was lifted off, leaving a section without film. The barren area was used to compare resistivity of the zinc to the silicon. The wafer was then placed in the cube furnace at 350°C for various times. The goal was to oxidize Zn until the resistivity measured $1x10^6$ (Ω/□) on a four point probe. Figure 4-6 outlines the experiment.

Time in Furnace	Resistivity
0 Minutes	100 Ω/□
10 Minutes	100 Ω/□
2 Hours	30×10^3 Ω/□
24 hours	1.5×10^6 Ω/□

Figure 4-6: Resistivity vs oxidation anneal time for a ZnO film with a film thickness of 250Å

When the time in the furnace reached 24 hours at 350°C a resistivity of 1.5×10^6 Ω/□ was measured. The oxidation process was then completed using a SAW device with 250 Å ZnO and 20 Å of Pd. Since the thickness of Pd is so low, the layer is considered discontinues, allowing the Zn to oxidize under the Pd. After completing the oxidation process, the ZnO sensors are ready for testing.

4.4 ZnO room temperature methane tests

This experiment sought to measure and observe changes in SAW amplitude when the sensor was exposed to methane gas at room temperature. The tested sensors were designed with a ZnO thin film and an ultra-thin film of Pd. The SAW's transducer was designed to operate at a center frequency of 50MHz. Three methane gas sensors were fabricated and tested at room temperature using the testing environment shown in figure 4-7.

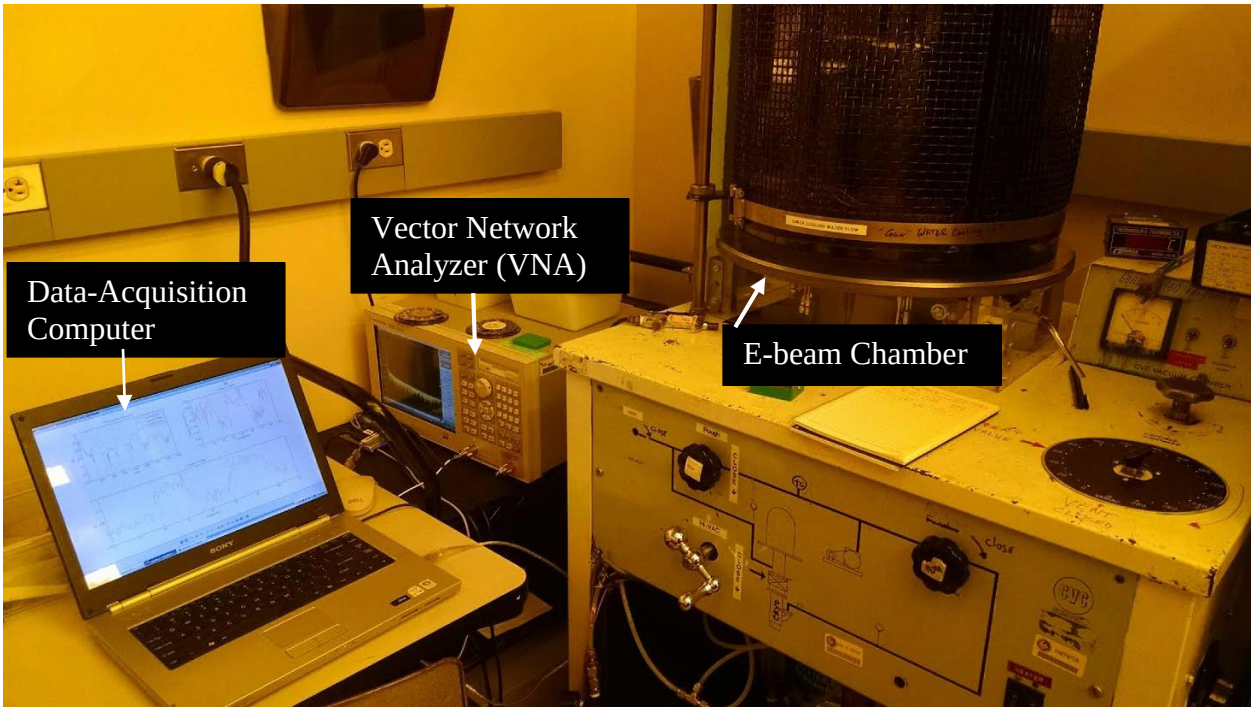

Figure 4-7: Methane gas testing equipment. The unit under test is connected to the vector network analyzer, which measures the scattering-parameters of the unit. The data is transferred to the data acquisition computer via USB. The data acquisition software programmed in MATLAB is used to measure the change in SAW propagation loss with gas concentration on the zinc oxide film.

Testing the methane sensor requires the following equipment; data-acquisition computer, vector network analyzer, and the device test fixture. The unit under test is connected to the vector network analyzer with a SMA connector. The VNA obtains data from the unit under test, in turn, transferring data to the data acquisition computer via USB. The data acquisition software programmed in MATLAB is used to interpret the data from the VNA, providing measurements on the SAW device. The software measures the S11 time response of the SAW, the differential change in group delay, and the change in SAW propagation loss. By observing a change in propagation loss a concentration of methane gas present at the film can be extracted from the data.

The measured data acquired from the acquisition software on sensor one is show in figure 4-8.

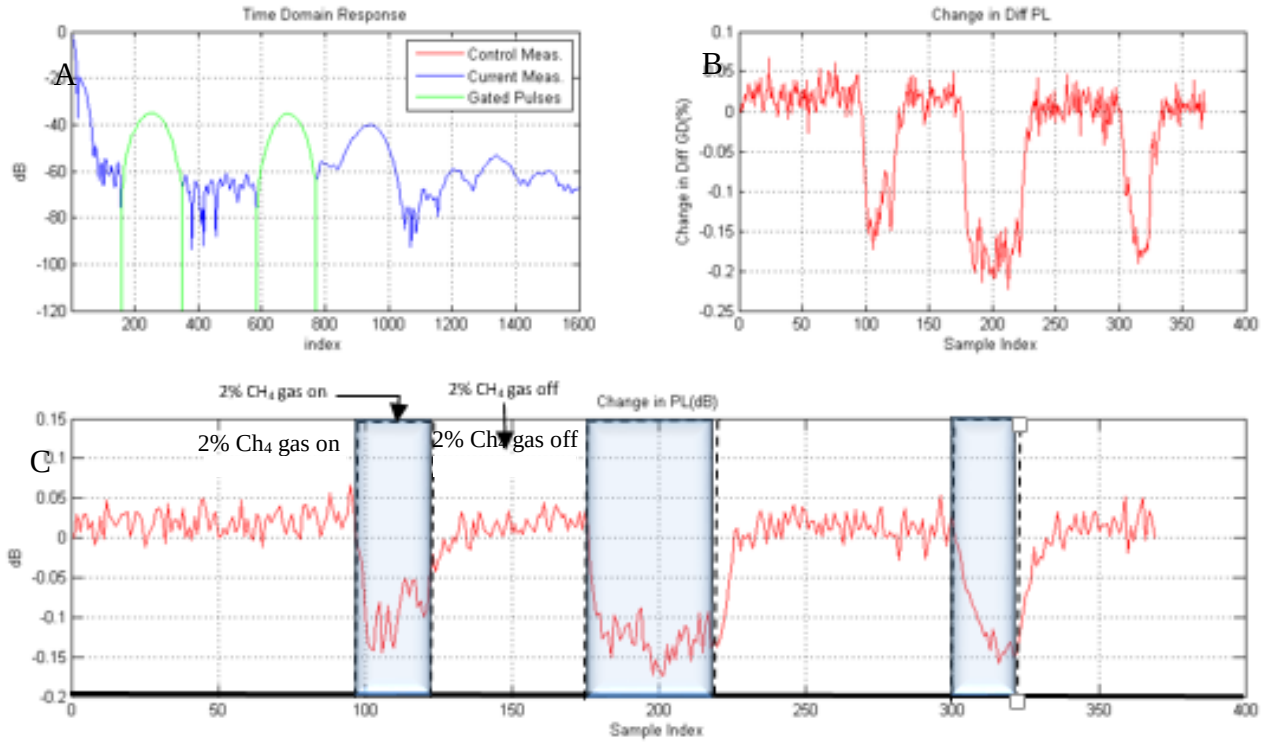

Figure 4-8: ZnO Methane sensor 1 tested at Room Temp; A) Time response of SAW for given instance, Control Meas. represents unaltered data, Current Meas. is the data effected by gas, Gate Pulses represents the portion of data being compared. B) Change in Group Delay. C) Change in differential pass loss with a blue overlay depicting gas exposures. Window C shows three observable changes in path loss when the CH_4 was present at the film. The max change in path loss observed was 0.15 dB.

The data-acquisition software outputted the plots where, window A provides a single measurement of the SAW device's time response. When viewed in real time the plot's peak amplitude varies as a function of gas concentration. Window B shows the measurement of the SAW's group delay versus the sample index. The sample index relates the number of samples over a given time, one sample is approximately 1 second. Lastly window C plots the change in path loss versus time. The blue overlays correlate to the portion of time in which gas is present at the film. According to window C, an observable change in propagation loss is measured for each

gas exposure. The change in dB was only 0.15 at the greatest point. It is believed that the small change in dB correlated to the blue overlays which signify a presence of methane gas. However, to fully determine if the sensors function, more sensors were fabricated and tested to bolster or deny the hypothesis.

The second sensor was fabricated and tested with no change in processes. This serves to recreate the first sensor experiment. The recorded data is shown in figure 4-9.

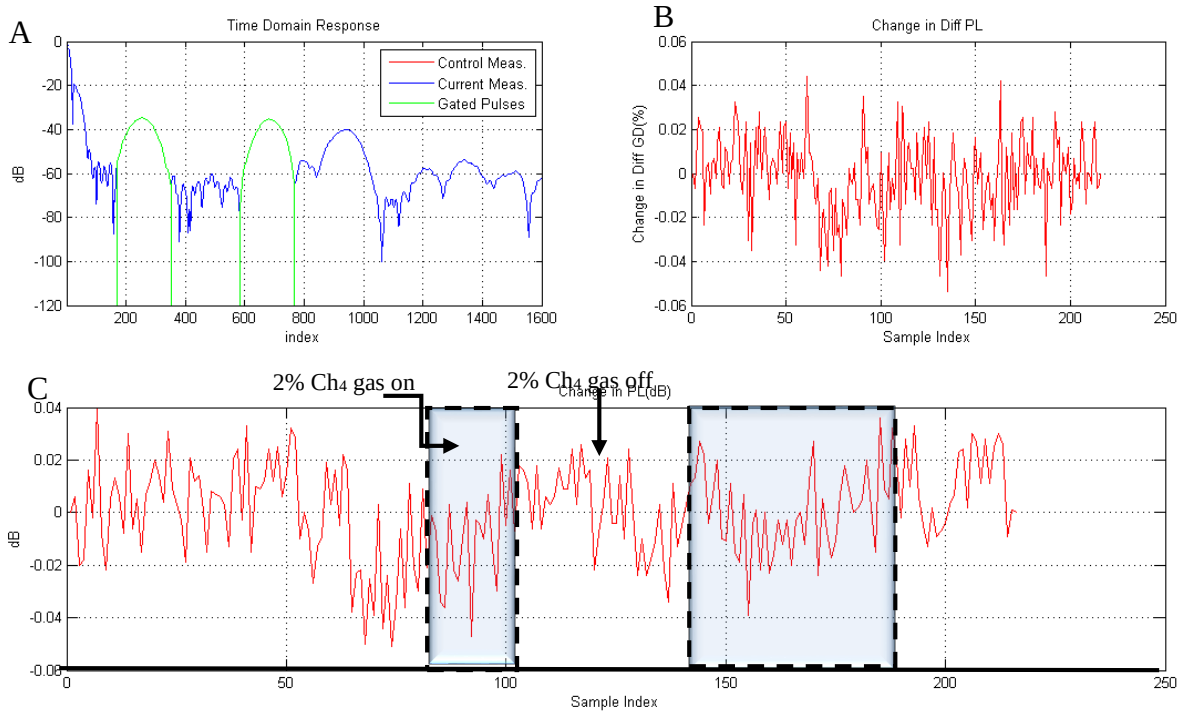

Figure 4-9: ZnO Methane sensor 2 tested at Room Temp; the change in differential pass loss varies time is shown in window C. The blue overlay depicts methane gas exposures. Window C shows no observable changes in path loss when the CH_4 was present at the film. The reason for failure is unknown.

The data acquired and outputted in the plots shows that, the sensor has no observable change in path loss when methane gas is applied at the film. Since no changes we made to the sensor fabrication process, a thickness measurement of the film was needed to determine if the deposition was successful. A film thickness of 50 Å was measured on the second sensor when using a dekteck profilimeter. 50 Å only accounts for palladium deposition on the substrate. Failure may be related to the film deposition. In order to test this hypothesis a third sensor was fabricated and tested.

The process for growing the oxide film on the third sensor was changed to test how a larger film width affected the deposition of material and gas absorption of the film. This was accomplished by extending the shadow mask's via width from 0.92mm to 1.49mm. The recorded data for the third sensor is shown in figure 4-10.

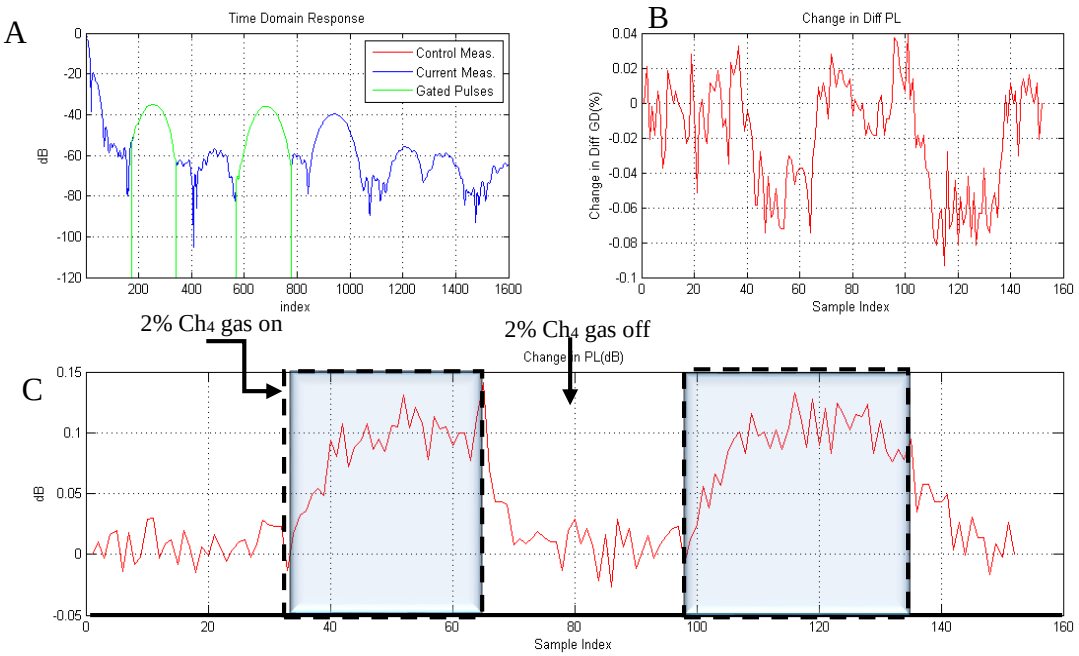

Figure 4-10: ZnO Methane sensor 3 tested at Room Temp; the change in differential pass loss varies time is shown in window C. The blue overlay depicts methane gas exposures. Window C shows two observable changes in path loss when the CH_4 was present at the film. The max change in path loss observed was 0.1 dB.

The data-acquisition software outputted the plots in figure 4-10, Window C plots the change in path loss when methane gas is present at the film versus time. The blue overlays correlate to the portion of time in which gas is present at the film. According to window C, an observable change in path loss is measured twice over the period of gas exposure. The change in dB was only 0.1 dB at the greatest point.

The observable path loss changes in dB occurred for both sensors one and three even though the deposition processes were different. Oddly sensor two failed even though its deposition process was the same as sensor one. I believe the inconsistent sensor results are related to the Zn deposition. Deposition rates of Zn during sensor fabrication were

uncontrollable, for this reason a stable deposition was never achieved. This lead to unexpected film thicknesses when measured using a profilimeter. In order to confirm or deny this hypothesis more sensors must be fabricated and tested.

4.5 ZnO Cross Sensitivity to H_2 at Room Temperature

The final experiment conducted determined whether zinc oxide experienced cross sensitivity to hydrogen gas. To produce this experiment sensor one was reused and was exposed to hydrogen gas. Before applying H_2 the gas line was purged of the remaining methane by flowing hydrogen through the test hose for 30 seconds. Figure 4-11 represents the data collected.

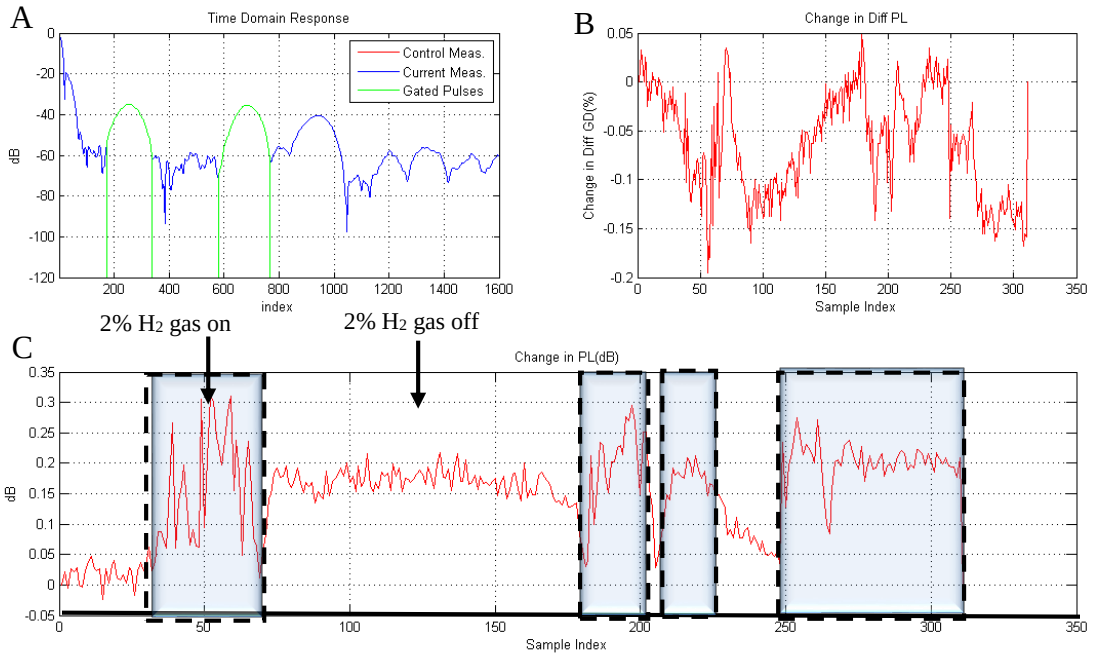

Figure 4-11: ZnO Methane sensor 1 tested for cross sensitivity to H_2 at Room Temp; the change in pass loss versus gas concentration is shown in window C. The blue overlay correlates to the hydrogen gas exposures. Window C shows four observable changes in path loss when the H_2 was present at the film. The max change in path loss observed was 0.3 dB.

The recorded data shows the ZnO device experiencing amplitude changes when H_2 is concentrated on the thin film at room temperature. Window C shows an observable change in path loss, which was measured four times. The first return time from 0.3 dB to 0 dB took 100 samples, which was much longer than the other 3 H_2 exposures. The sensor's max change in amplitude was 0.3 dB. Based on the observable changes in amplitude an H_2 concentration at the film is believed to affect the path loss. This shows the possibility of H_2 cross sensitivity. Testing this hypothesis requires more sensors to be fabricated and tested. Also further experiments must be created to determine methods to of designating between the H_2 and CH_4.

Chapter 5 Conclusion

Using a surface acoustic wave delay line combined with the proper thin film has shown possible reactions to the presence of gas at the thin film. Gas sensing is achieved by altering the acoustoelectric losses through changes in the propagation path resistance. Measurements were conducted using the test fixtures presented in chapter 4. Exposing a ZnO thin-film to CH_4 gas produced observable changes in SAW propagation loss. The change in path loss was recorded using the data acquisition software described in chapter 4. Unfortunately a less than desirable change in path loss was measured for each responsive sensor. The maximum recorded change in path loss was 0.15 dB. This change in dB is considerably low when compared to SnO_2 hydrogen gas sensors [5].

The ZnO thin-film used has shown reusability when tested multiple times at room temperature, represented as the absorption and desorption of gas into the film. This process occurred when the methane gas' presence at the film was removed or applied. The recorded data from each sensor showed the change in path loss returning to zero dB multiple times in a single experiment. However, the time it took for the sensors to return to zero dB varied for each device. It is believed that the deportation and absorption rates are directly related to the thickness of the thin-film. Therefore more experiments must be conducted to confirm or deny this hypothesis.

The experimental data recorded on a ZnO film has shown cross sensitivity to hydrogen gas at room temperature. Since the sensors reacted to hydrogen gas a method must be developed to distinguish between H_2 and CH_4. SnO_2 is known to not react with methane gas at room temperature when using a SAW delay line device [5]. Having both ZnO and SnO_2 films on the

substrate is a possible method to analyze cross sensitivity. By placing one film per propagation path, only one transit experiences a change in path loss when methane is present while both transits encounter changes in path loss when hydrogen presence. However confirming or denying this relationship would require development of newer test fixtures to deposit films.

Unfortunately using ZnO has not shown to be an effective method of sensing methane gas at room temperature. The recorded reactions to methane gas are skewed by the chance of experimental error. This is because the sensors did not provide a suitable change in dB to eliminate possible outside effects. I believe that a change in 0.15dB does not provide enough evidence to support a reaction based solely on the presence of methane gas. More research must be conducted to determine the cause of unsatisfactory devices. The suspected cause of failure is film deposition, I believe the ZnO film quality was too poor to react with methane gas. This hypothesis is based on the highly uncontrollable and unpredictable nature of my Zn depositions. During E-beam depositions, Zn evaporated at lower currents but had an uncontrollable deposition rate. This made it near impossible to match the predicted film thickness to the measured thickness. Better methods of depositing ZnO must be devised. With the completion of this research further work can be conducted to develop a better room temperature methane sensor using ZnO. Better processing techniques must be devised to grow a high quality film on the SAW. Upon reproducible testing of a 50 MHz sensor methane sensitivity on 915 MHz devices will be explored. 915 MHz devices should provide a much greater change path loss of the SAW, if they function similarly to hydrogen sensors at the same frequency. Lastly, when properly developed these sensors can prevent and warn of methane gas leaks.

Appendix A

Process Flow:

SAW Fabrication:

Wafer Fabrication

University of Central Florida

College of Engineering

Electrical Engineering Department

SAW Sensor

Joseph Serritella

Procedure:

I. **Retrieve hot plate from storage and place in photolithography room. Set the plate to 100 degrees C**

II. **Check if Nitrogen to the clean room is turned on**

III. **Set up Mask Aligner**

a. Switch on compressed air and Nitrogen

i. The switches are located to the left of the gauges

b. Switch on the vacuum line

i. The power cord is to the left of the mask aligner

c. Switch on the power using the button located on the console

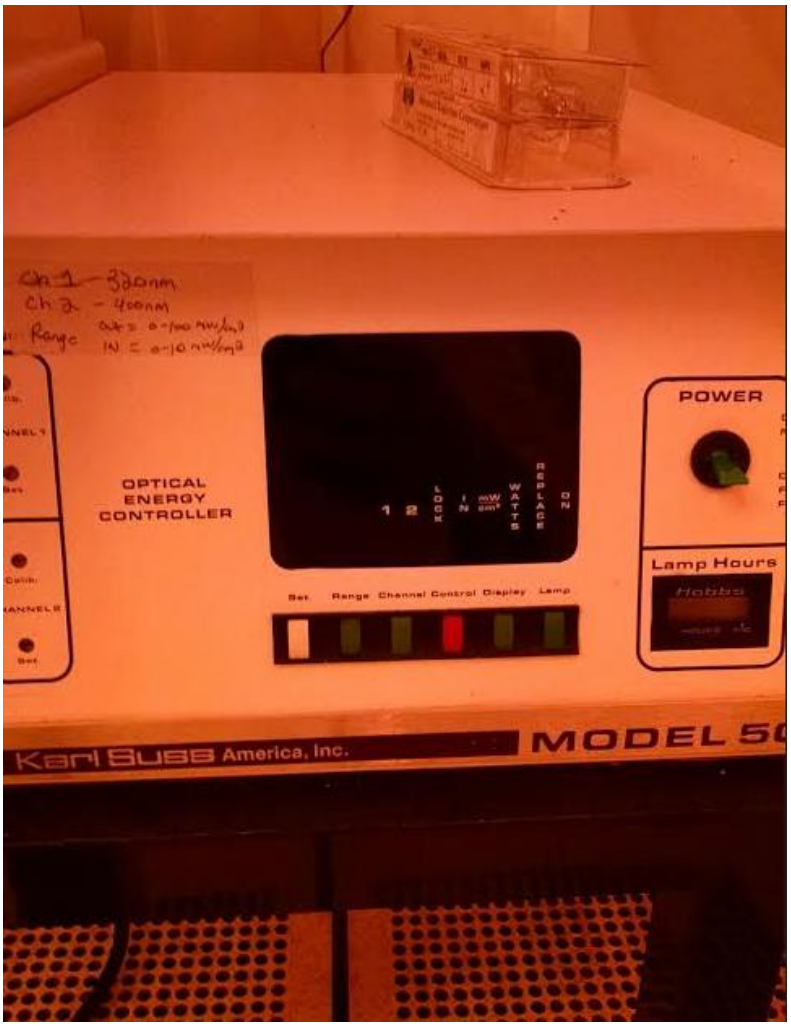

i. Turn on green toggle

ii. Control is pushed out (light is off)

iii. Press lamp

iv. Fill in the sign in sheet

IV. Obtain wafers from storage and clean the wafer

V. Photolithography process

a. Test the spinner using a quartz wafer

i. Set to 4000 RPM for 40 Seconds

b. Place the ready wafer onto the vacuum chuck and center

i. Make sure to place wafer correctly

c. Apply HMDS to the wafer

i. HMDS is to help with the adhesion of the PR

d. Spin the wafer

e. Apply BPRS 100 to the wafer

i. Be sure to spread out PR and let the PR settle

f. Spin the wafer

g. Bake on Hot plate for 90 seconds

VI. Mask Aligner

a. Retrieve the light meter and place on vacuum chuck

b. Expose for 30 seconds

i. Measure at 365 nm and 400 nm

c. Obtain the required mask for the process

d. Place the mask on the chuck (copper face down) fingers parallel to the edge of the housing

i. Align the wafer to the edge of the chuck

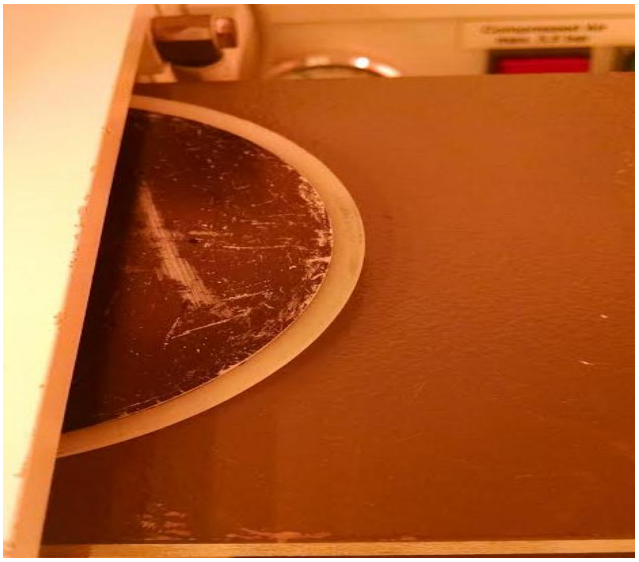

ii. Tighten down the mask knobs

iii. Put the mask into contact

1. Make sure light is on

e. Expose the wafer for 30 seconds

f. Remove wafer

VII. Developer

a. Use a glass petri dish

i. Use “Malocha PLSI” for positive PR

ii. Use a second glass petri dish for a stop bath

iii. Place the wafer into the developer

1. Process takes approximately 30 seconds

iv. Clean with DI water and Dry

v. Inspect under the microscope for impurities

1. Re work if needed

vi. Plasma clean the wafer

VIII. Deposition

- **a.** Use appendix B and C

IX. Lift off

- **a.** Retrieve the sonic bath
- **b.** Fill beaker with water and pour into the sonic bath
    - **i.** About half way to operating level
- **c.** Pour acetone into a glass petri dish and place wafer into the dish
- **d.** Turn on the sonic bath
- **e.** Use visuals to determine when the film has lifted off
- **f.** Rinse with DI water and dry

Appendix B

Process Flow:

Hydrogen/Methane Sensor Thin Film Deposition:

Electron beam Vacuum operation

University of Central Florida

College of Engineering

Electrical Engineering Department

SAW Sensor

Joseph Serritella

Procedure:

X. E-Beam Checklist

a. Check Flow Meters

i. Crystal monitor should read approximately 0.25 Gallons per minute. The crystal monitor is located to the right of the lower storage area

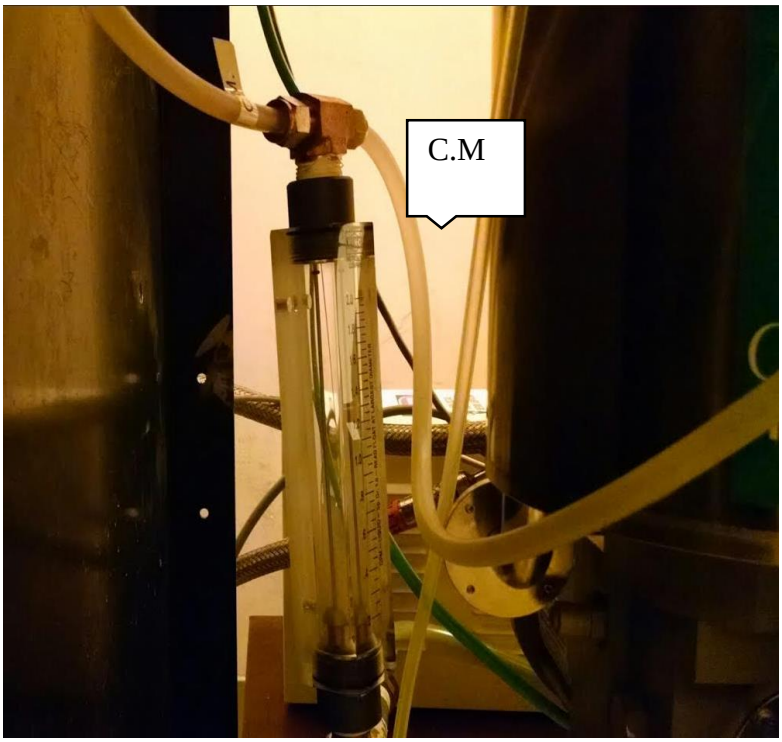

ii. While to the left is the Gun Flow reader. Normal should read 0.50 Gallons per minute.

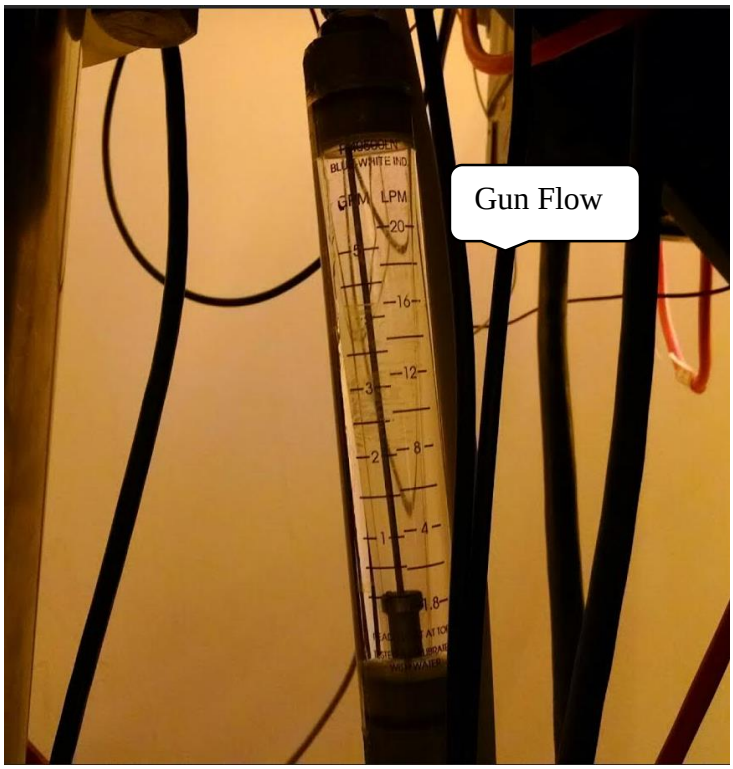

b. Inspect the Cryo for optimal running temperature (T <= 15 K)

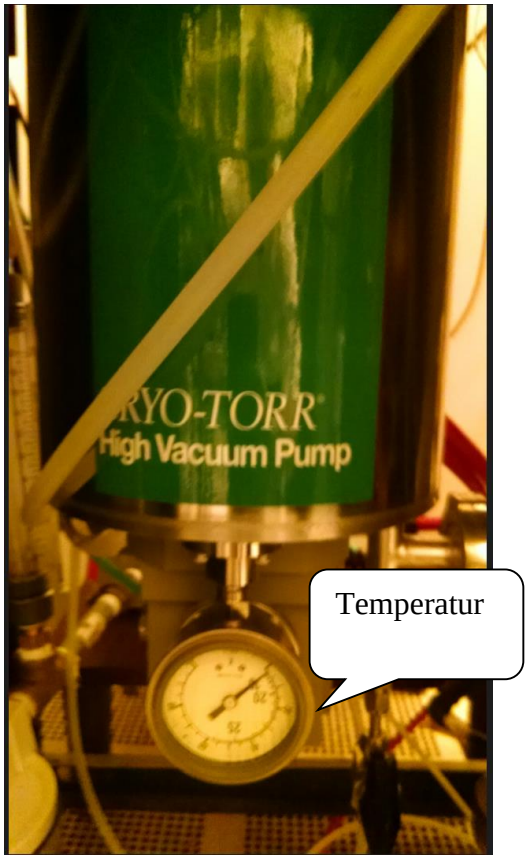

c. Vent the E-beam's Bell Chamber by turning valve located next to the chamber. Turn valve all the way. Wait until the chamber is at atmospheric pressure. A hissing sound will indicate that the chamber has reached atmosphere.

i. Please note, if cryo pump is sweating or above 15 K do not continue.

d. Close the Vent and lift the Bell Chamber.

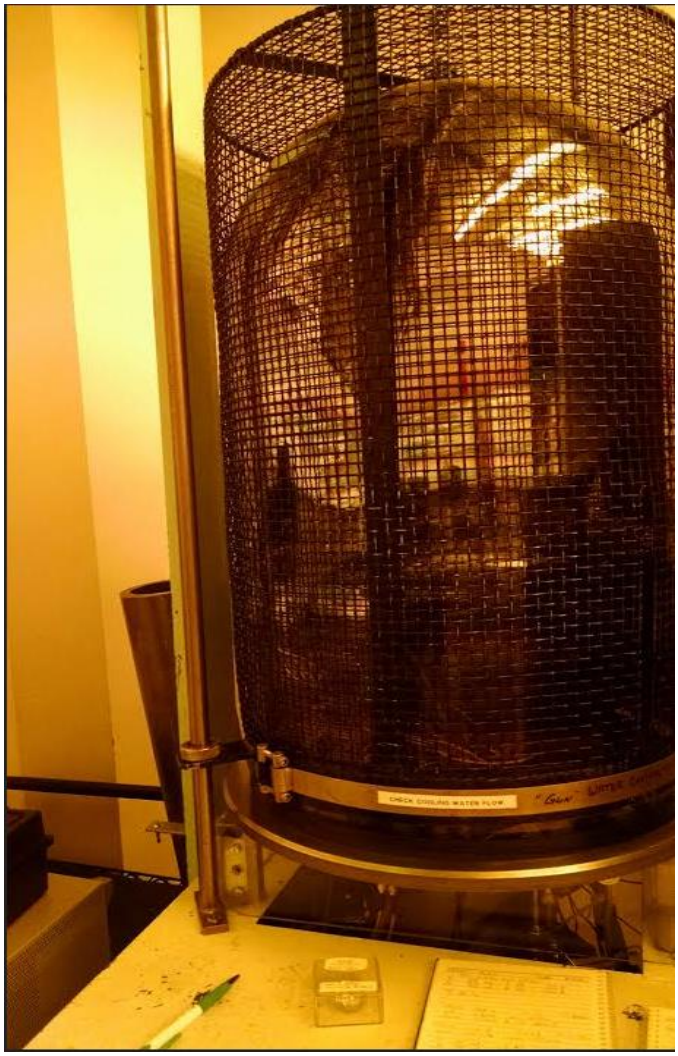

XI. Pump-Down over view

a. In order to be pumped down there are several valves that need to be located and explained.

i. When approached the E-Beam will be in the stand-by state which consist of all

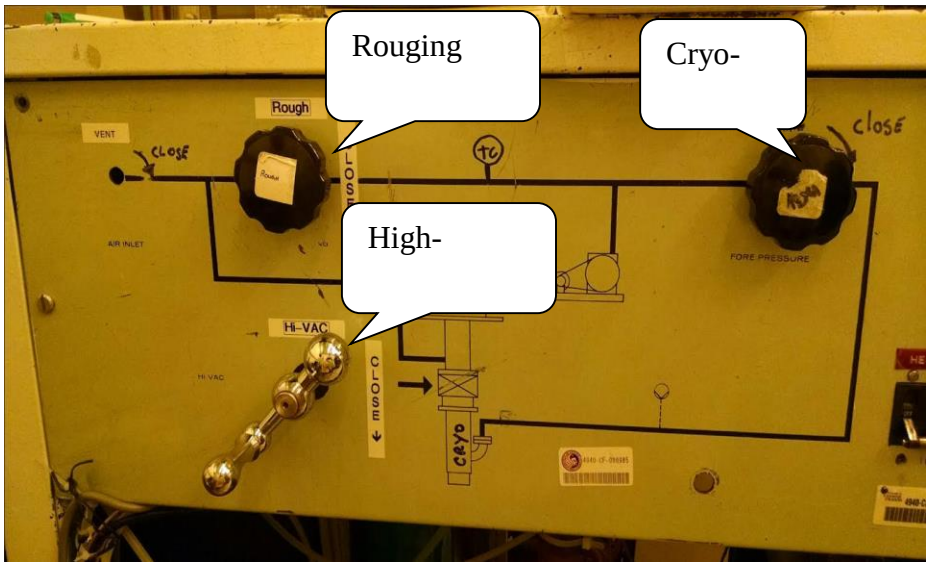

b. The rouging valve controls the initial pumping state of the e-beam chamber. This is used to remove large particles the high vacuum pump cannot handle. Typical pressure is from atmosphere to 50 MicroTorr

c. High-vacuum valve remains closed while the roughing valve is open. This valve allows the Cryo-Torr pump access to the chamber. This is used to remove most all particles the roughing vacuum pump cannot remove. Typical pressure is from 50 MicroTorr to 3 MicroTorr

d. Finally, the regen valve is only opened for cryo regen.

e. Below is a table listing e-beam states. X=Closed O=Open

STATE	ROUGHING	HIGH_VAC	VENT	REGEN	SOLENOID
STANDBY	**X**	**X**	**X**	**X**	**X**
ROUGH	**O**	**X**	**X**	**X**	**X**
HIGH VAC	**X**	**O**	**X**	**X**	**X**
VENT	**X**	**X**	**O**	**X**	**X**
REGEN	**X**	**X**	**X**	**O**	**O**

f. Turn on the roughing, followed by turning on the pressure gauges located on the server rack next to the E-beam.

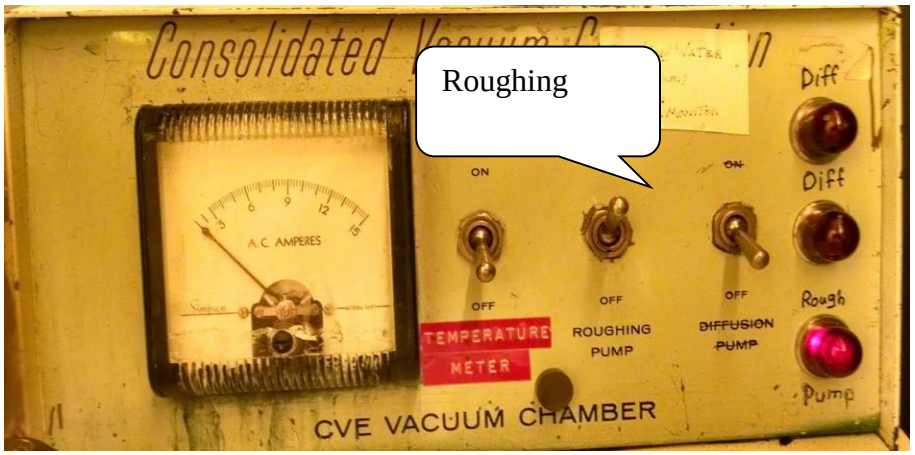

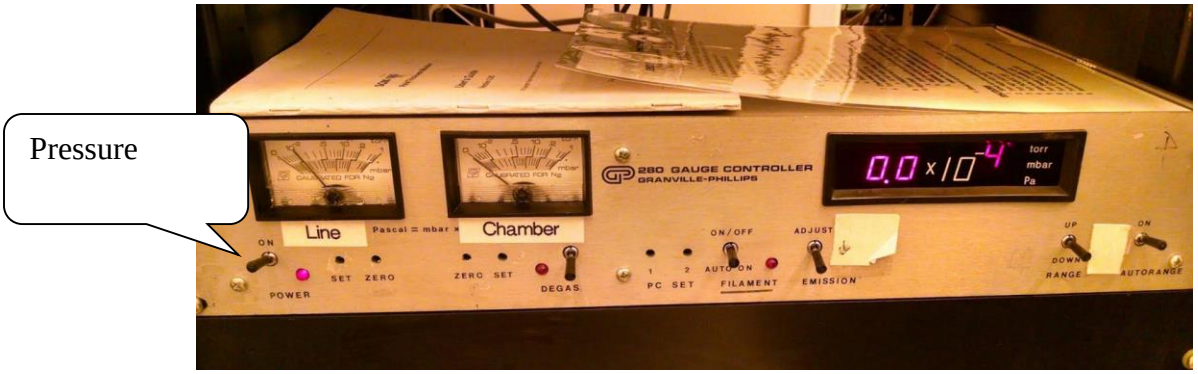

g. Power the Crystal monitor to keep track of pump times.

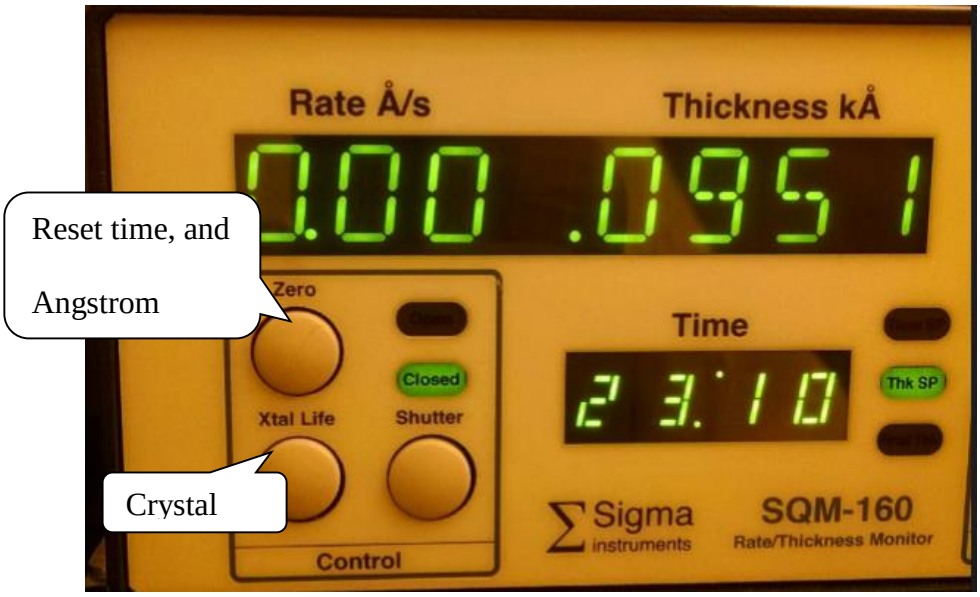

h. Turn on the Crystal monitor and press **"ZERO"**

i. MAKE SURE VENT VALVE IS CLOSED

1. Depicted below is the vent valve in the closed position

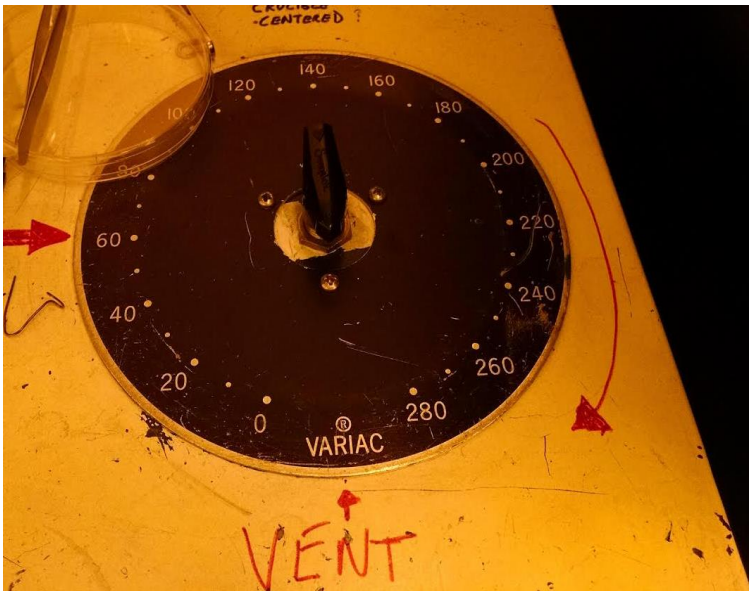

XII. Roughing state

a. Open the roughing valve all the way and give a quarter turn back.

b. Roughing is complete when the chamber pressure reaches 50 MicroTorr

c. Closely monitor the chamber pressure, until the reader reaches 50 MicroTorr.

d. Once appropriate pressure has been reached close the roughing valve tightly. The approximate time for roughing is 8 minutes and 30 seconds.

i. Note, times will vary based on vacuum.

XIII. High-Vacuum state

a. Being by slowly turning the high-vacuum valve for two revolutions. Then going faster each revolution until the chamber pressure starts to drop.

b. When the pressure is off scale toggle the Ionization gauge.

i. The Ionization gauge is triggered by toggling the filament switch up

c. Pump down until the chamber reaches 3 MicroTorr or stop when the crystal monitor timer reaches 20 minutes.

i. If the pump down is taking exceeding long check for leaks by applying methanol to possible leak zones around the bell chamber.

1. A common leak may be from the vent valve

ii. Once the complete toggle the ionization gauge filament off.

XIV. Venting State

a. In order to remove the samples from the chamber the chamber must be vented. In order to vent make sure all valves are closed. Once closed turn the valve to the open position

b. By opening the vent valve the chamber will be purged with nitrogen and brought back to atmosphere.

i. Purge is complete when a large audible hissing is heard.

c. Close the vent valve and remove samples.

d. If the High Vacuum valve is open during venting please refer to the regen section.

XV. Cryo Regeneration

a. Cryo Regeneration is a result of the Cryo-Torr high vacuum pump being bombed. Causes for this are as follows.

i. Venting while high-vac valve is open.

1. Bombing is made worst when chamber is open for long exposing the cyro-torr to the atmosphere

ii. Roughing open while high-vac valve is open

iii. In case of bombing turn off the air compressor located to the left of the e-beam near the floor.

iv. Close high-vac valve.

v. Symptoms

1. Cryo starts to condensate.

2. Cryo Temperature exceeds normal 15 K

b. In order to regen the cryo, verify line pressure has dropped on the server rack.

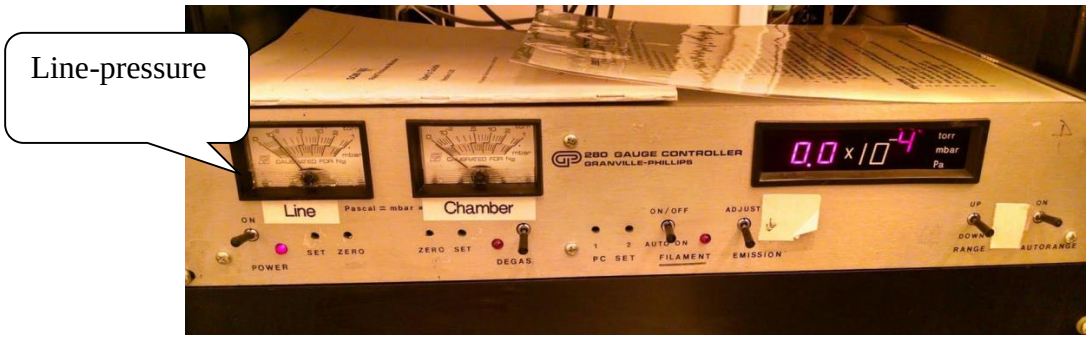

a. Open the roughing valve and pump down for 6 minutes, followed by opening the regen valve.

b. Close the Roughing pump, and located the power cord the cryo's solenoid valve and plug into the nearest power strip.

c. Pump down the cryo for approximately one full day.

Appendix C

Process Flow:

Hydrogen/Methane Sensor Thin Film Deposition:

Electron beam Deposition

University of Central Florida

College of Engineering

Electrical Engineering Department

SAW Sensor

Joseph Serritella

Procedure:

I. Running the E-beam

a. After the chamber is at vacuum (procdure is in appendix: Electron Beam vacuum operation) flip the breaker power up and let warm for 3 minutes

b. When ready the LED light (AIR CAB) will be illuminated. Also the LED's for VAC, Tank, HVAC, H_2O, and AUX2 and so on will be illuminated.

c. To continue in the deposition process the key for AUX 1 must be in the on position.

i. Visual of LED's

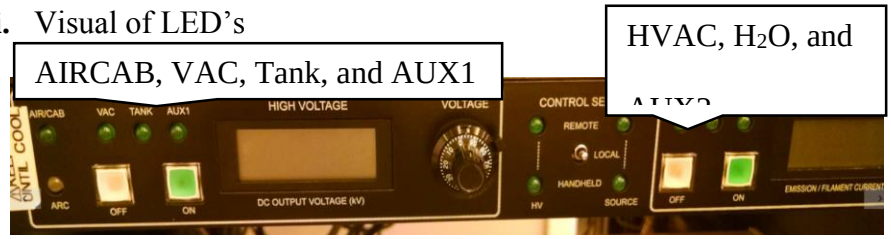

d. Turn on Control power and the sweep controller. These switches are located on the server rack.

e. Turn the source on, making sure the the EMS is flipped up, once the LCD reader is between 18-20 mA (~1min) flip the EMS to FIL.

f. Turn on the High Voltage and do not turn the dial, it will read 8 KV standard.

II. Crystal monitor startup

a. Make sure the crystal monitor is powered up. A power switch is located on the back of the device.

b. Check the crystal monitor for the correct settings for SnO_2 and Pd in both Xmontior 1 and Xmonitor 2. The valves for the density and Z-factor are located in a booklet on top of the crystal monitor

i. Note there is no display for Tin Dioxide (SnO_2) so you must alter Gold's (Au) settings

ii. Palladium's (Pd) settings will be located under Pd. Don't not alter any other setting.

iii. Xmontior 1 and Xmonitor 2 correspond to the location of the crystal monitor being used. 1 is for pre-deposition and 2 is for deposition.

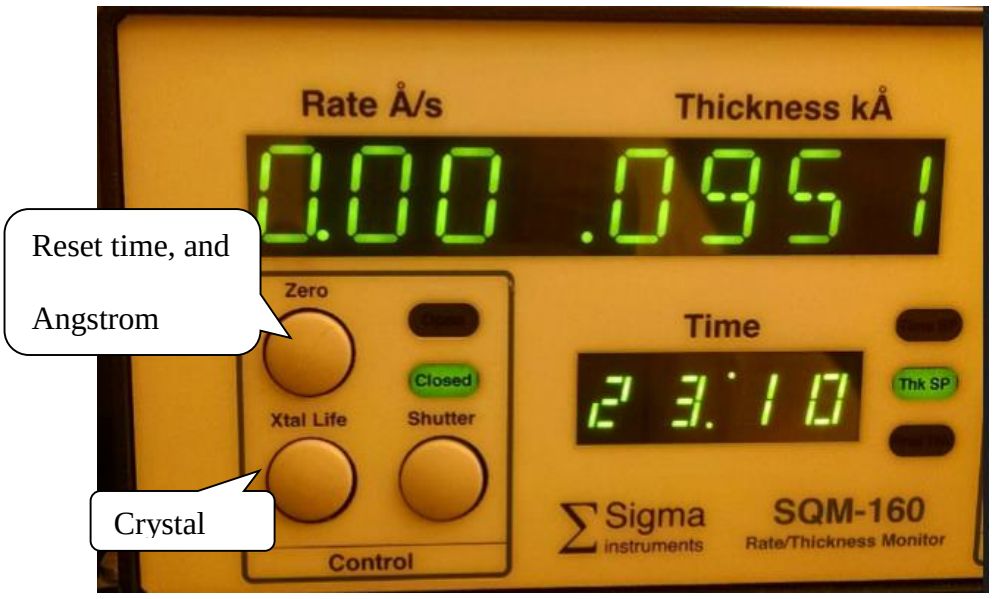

III. SnO_2 Pre-Deposition

a. Make sure the current metal is set to SnO_2 (if not this is covered in appendix: crucible loading and gun operation)

b. Turn the filament dial slowly until the SnO_2 is glowing and starts to evaporate. Increasing the amperes will increase the rate of evaporation

i. Make sure to place the beam in the center of the curable and not at all touching the edge of the liner.

1. There are patterns that can be used with the sweep controller, make sure if using spiral or triangle that the amplitudes don't cause it to extend out the crucible

ii. SnO_2 sublimes so it will start to evaporate at around 6mA extremely fast.

c. Once a good dep-rate of 3 Angstroms per second is reached we are ready to start the deposition.

i. Note the pre-dep rate is three time that of the dep rate

IV. SnO_2 Deposition

a. Zero the crystal monitor and remove the shutter from protecting the sample.

i. Note that removing the shutter may cause the rate to go negative; this is from a change in temperature and is normal.

b. Based on the desired thickness times may change

c. For Hydrogen sensors the thickness of SnO_2 should be approximately 250 Angstroms at 1 Angstroms per second.

d. When the monitor reaches near the desired thickness close the shutter and thus stopping the deposition.

e. Slowly turn the filament dial down allowing the crucible to cool properly

V. Pd Pre-Dep

a. Now that SnO_2 is complete turn the gun to the desired location of Pd.

i. Make sure to only turn the gun right, going left may loosen the chain. (Covered in more detail in appendix: gun operation)

b. Turn the filament dial slowly until the Pd is glowing and starts to evaporate. Increasing the amperes will increase the rate of evaporation

i. Pd does not sublime so it will start to evaporate at around 25mA~35mA

1. Higher current corresponds to higher dep rate.

2. There are patterns that can be used with the sweep controller, make sure if using spiral or triangle that the amplitudes don't cause it to extend out the crucible

c. Once a good dep-rate of 0.3 Angstroms per second is reached we are ready to start the deposition.

i. Note the pre-dep rate is three time of the dep rate

VI. Pd deposition

a. Zero the crystal monitor and remove the shutter from protecting the sample.

i. Note that removing the shutter may cause the rate to go negative; this is from a change in temperature and is normal.

b. Based on the desired thickness times may change

c. For Hydrogen sensors the thickness of our Pd should be approximately 20 Angstroms at 0.10 Angstroms per second.

d. When the monitor reaches near the desired thickness close the shutter and thus stopping the deposition.

e. Slowly turn the filament dial down allowing the crucible to cool properly

VII. Sample Removal

a. Once the crucible has cooled down and the filament has be dialed down to the lowest place begin the powering down.

b. Start by turning off the High voltage and the source off, Turn the AUX 1 key to the off position

c. Zero the timer on the X monitor and wait 5 minutes before turning off the sweep controller and controller power.

d. Close the High VAC valve.

  i. Note: don't close high vacuum valve until the high voltage is turned off. This may cause arcing in the chamber.

e. Once 5 minutes has been reached turn off the Sweep Controller, and Controller power. Then you must flip off the breaker.

f. It is now safe to vent the chamber and remove the sample

g. Once the sample and test fixture is removed (this is covered in appendix: Loading the E-beam) place the planetary back into the bell chamber.

h. Close the Bell chamber and open the roughing pump.

i. Pump down to stand-by pressure (50 microTorr) and close the roughing valve. The E-beam is in stand-by

List of References

[1] G. Tournier, C. Pijolat, R. Lalauze, and B. Patissier ," Selective detection of CO and CH_4 with gas sensors using SnO_2 doped with palladium," Sensors and Actuators, Vol. B, no. 26-27, 24-28, 1995.

[2] P. Bhattacharyya, P.K. Basu, H. Saha, and S. Basu, " Fast response methane sensor using nanocrystalline zinc oxide thin films derived by sol-gel method," Sensor and Actuators, Vol. B, no. 124, 62-67, January 2007.

[3] D. Gruber, F. Kraus and J. Muller, " A novel gas sensor design based on $CH_4/H_2/H_2O$ plasma etched ZnO Thin films," Sensors and Actuators, Vol. B, no. 92, 81-89, January 2003.

[4] Wolfgang Gopel, Klaus Schierbaum, "SnO_2 sensors: current status and future prospects," Sensors and Actuators B, vol. 26, Issue 1-3, pp. 1-12, 1995.

[5] B. H Fisher, "Surface acoustic wave (saw) cryogenic liquid and hydrogen gas sensor," UCF 2012, published 2012.

[6] D. Morgan, Surface Acoustic Wave Filters: With Application to Electronic Communications and Signal Processing, 2nd ed. Boston: Elsevier, 2007.

[7] K. A. Ingebrigtsen, "Linear and Nonlinear Attenuation of Acoustic Surface Waves in a Piezoelectric Coated with a Semiconducting Film," Journal of Applied Physics, vol. 41, pp. 454-459, 1970.

[8] B. H. Fisher and D. C. Malocha, "Room Temperature Hydrogen Gas Sensing Using SAW Devices," JSPS and IEEE UFFC Society International Acoustic Devices Conference, 2008.

[9] T. Xu, M. P. Zach, Z. L. Xiao, D. Rosenmann, U. Welp, W. K. Kwok, and G. W. Crabtree, "Self-assembled monolayer-enhanced hydrogen sensing with ultrathin palladium films," Applied Physics Letters, vol. 86, pp. 203104, 2005.

[10] D. H. Piehl, "Oxidation of aluminum foil under simulated high temperature annealing using thermogravimetry," *Journal of Thermal Analysis*, vol. 6, p. 9, 1974.